**Electronic Supplementary Information**

# A versatile molecular logic system based on Eu(III) coordination polymer film electrodes combined with multiple properties of NADH

Wenting Wei,[a] Jiaxuan Li,[a] Huiqin Yao,[b] Keren Shi,[c] Hongyun Liu[a] *

[a] Key Laboratory of Radiopharmaceuticals, Ministry of Education, College of Chemistry, Beijing Normal University, Beijing 100875, People's Republic of China

[b] School of Basic Medicine, Ningxia Medical University, Yinchuan 750004, People's Republic of China

[c] State Key Laboratory of High-efficiency Utilization of Coal and Green Chemical Engineering, Ningxia, Yinchuan 750021, People's Republic of China

*Corresponding author: Hongyun Liu, 19, Xinjiekouwai Street, Haidian District, Beijing 100875, People's Republic of China. Tel: (86)-10-58807843. E-mail: liuhongyun@bnu.edu.cn.

### 3.1 Characterization of Eu(III)-PMAG films

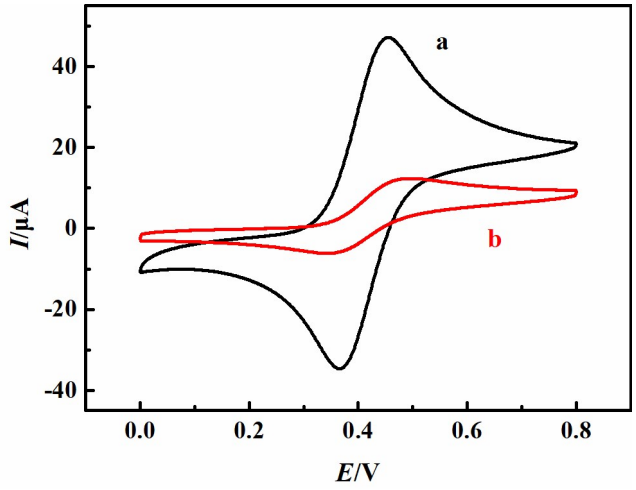


**Fig. S1** CVs of 0.5 mM FcDA at 0.05 V $s^{-1}$ in pH 5.0 buffers at (a) ITO and (b) Eu(III)-PMAG film electrodes.

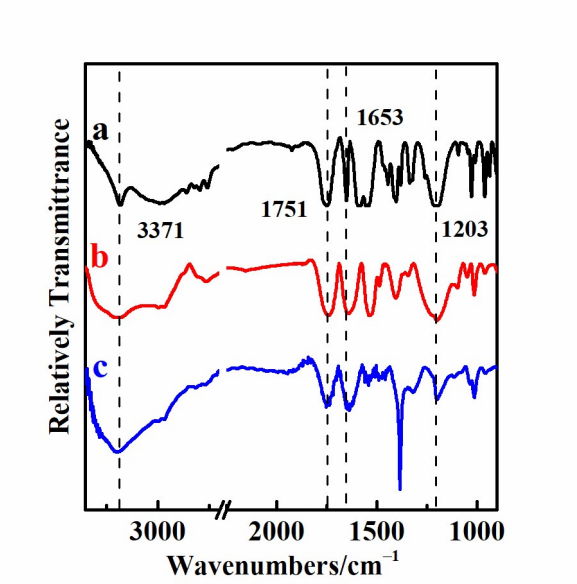


**Fig. S2** FTIR spectra of (a) MAG, (b) PMAG and (c) Eu(III)-PMAG samples.

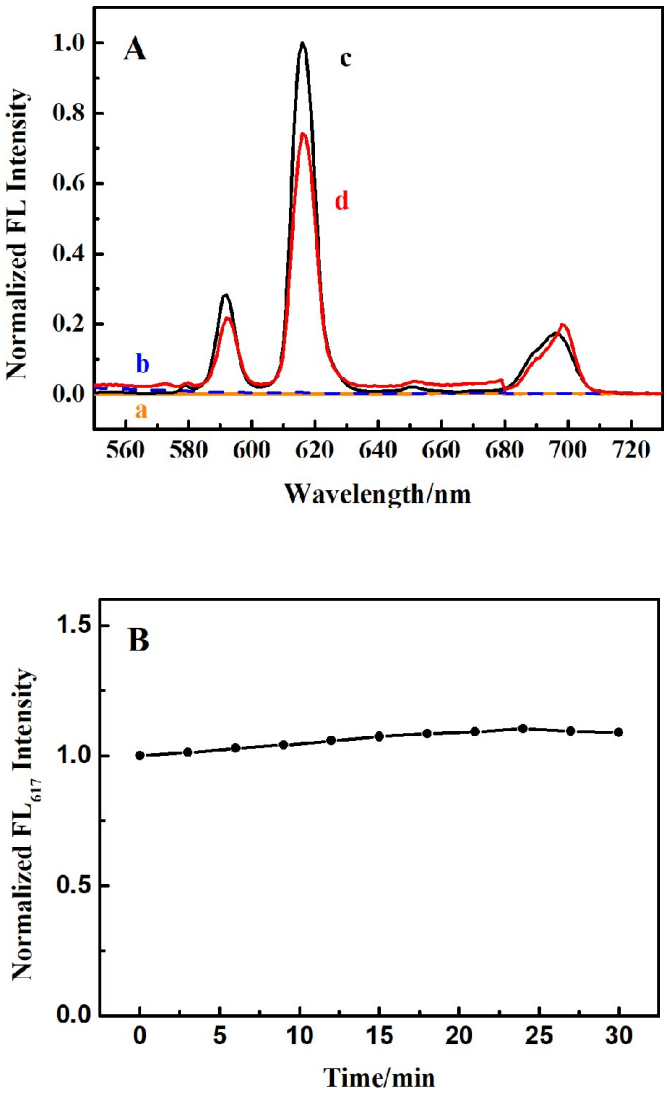


**Fig. S3** (A) FL emission spectra for (a) bare ITO, (b) dry PMAG films, (c) dry Eu(III)-PMAG films and (d) Eu(III)-PMAG films in pH 5.0 buffers. (B) Dependence of the $FL_{617}$ intensity for Eu(III)-PMAG films upon immersion time in pH 5.0 buffers.

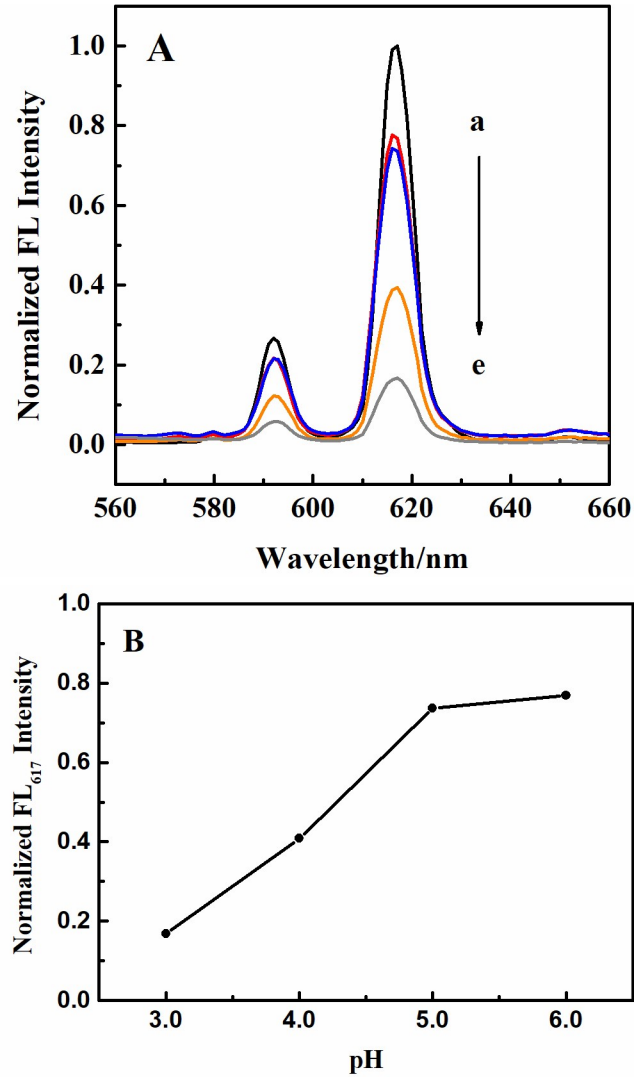


**Fig. S4** (A) FL spectra of (a) dry Eu(III)-PMAG films and Eu(III)-PMAG films in buffers at pH (b) 6.0, (c) 5.0, (d) 4.0 and (e) 3.0. (B) Dependence of the $FL_{617}$ intensity for Eu(III)-PMAG films upon different pHs.

### 3.2 Cu(II)-sensitive FL for Eu(III)-PMAG films

Compared with the Eu(III)-PMAG film electrodes before the immersion in Cu(II) solution (Fig. S5A, curve a), an obvious $Cu2p_{3/2}$ XPS peak was observed after the immersion of the film electrodes in 5 mM Cu(II) solution (Fig. S5A, curve b), indicating that Cu(II) indeed coordinated with PMAG films. Moreover, the average binding energy of $Cu2p_{3/2}$ for the Eu(III)-PMAG samples after the interaction with Cu(II) (933.32 eV) reduced by 0.93 eV compared with the copper acetate powder sample (934.25 eV) (Fig. S5A, curve c). At the same time, the average binding energy of $Eu3d_{5/2}$ in Eu(III)-PMAG sample (1135.42 eV) increased by 0.87 eV after the immersion in the Cu(II) solution (1136.29 eV) (Fig. S5B). These results suggested that the coordination of Cu(II) with the N and O atoms of PMAG in the films increased the electron density of Cu(II). In addition, the coordination of Cu(II) with PMAG affected the coordination action of Eu(III) ions, which changed the coordination environment around Eu(III) and PMAG and reduced the electron density of Eu(III). All of these supported that Cu(II) could coordinate with PMAG films and further affect the luminescent behavior of Eu(III)-PMAG films.

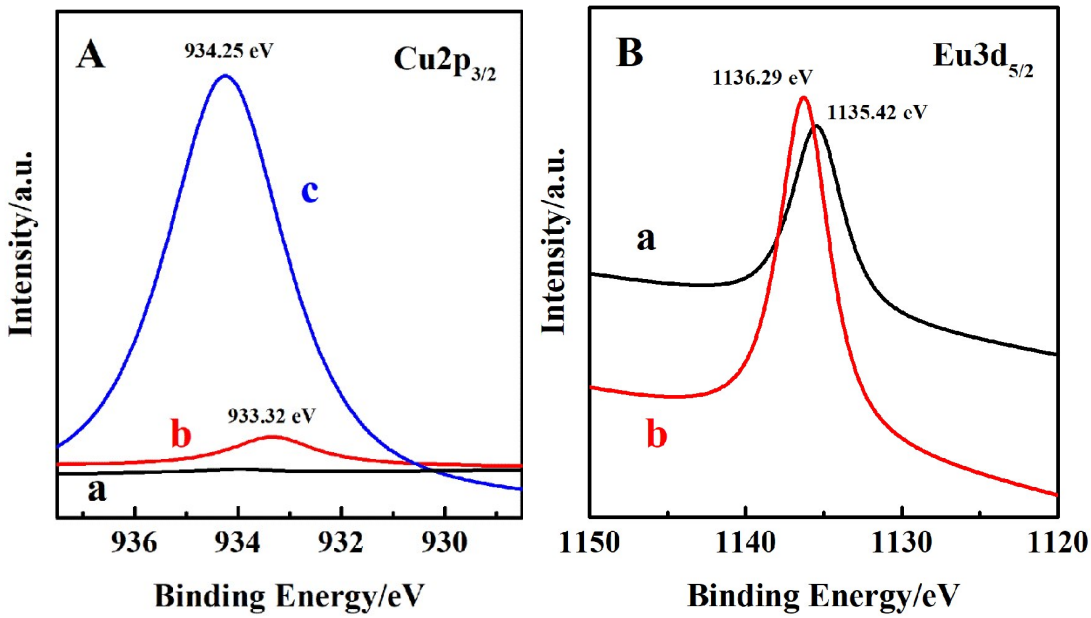


**Fig. S5** (A) XPS spectra of $Cu2p_{3/2}$ for Eu(III)-PMAG film electrodes (a) before and (b) after immersing in pH 5.0 solution containing 5.0 mM Cu(II), and (c) $Cu(CH_3COO)_2 \cdot H_2O$ powder. (B) XPS spectra of $Eu3d_{5/2}$ for Eu(III)-PMAG film electrodes (a) before and (b) after immersing in pH 5.0 solution containing 5.0 mM Cu(II).

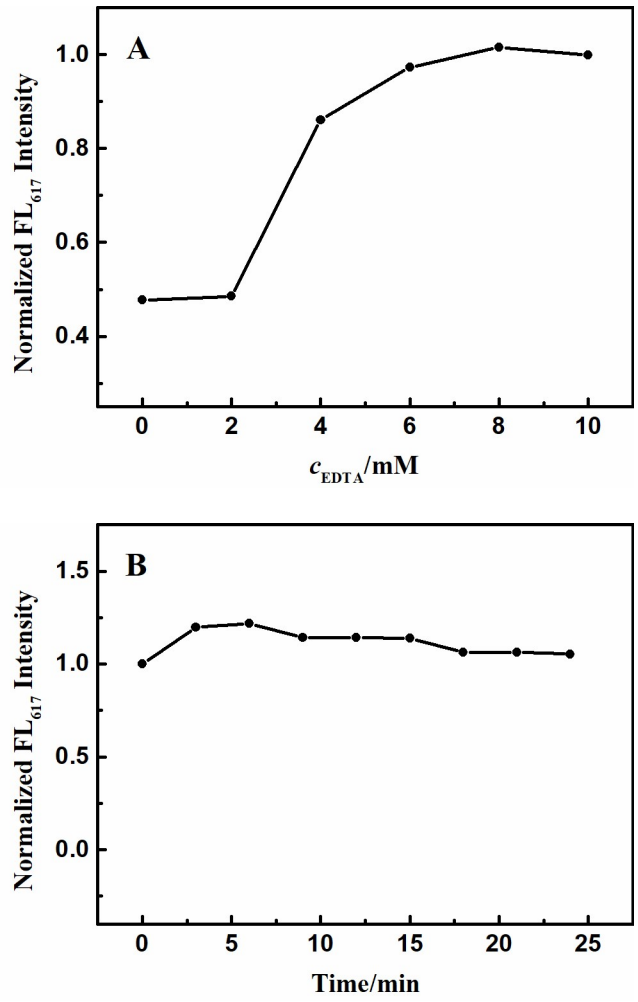


**Fig. S6** (A) Dependence of the $FL_{617}$ for Eu(III)-PMAG films after immersion in pH 5.0 buffers containing 5.0 mM Cu(II) upon different EDTA concentrations. (B) Dependence of the $FL_{617}$ for Eu(III)-PMAG films upon immersion time in pH 5.0 buffers containing 8.0 mM EDTA.

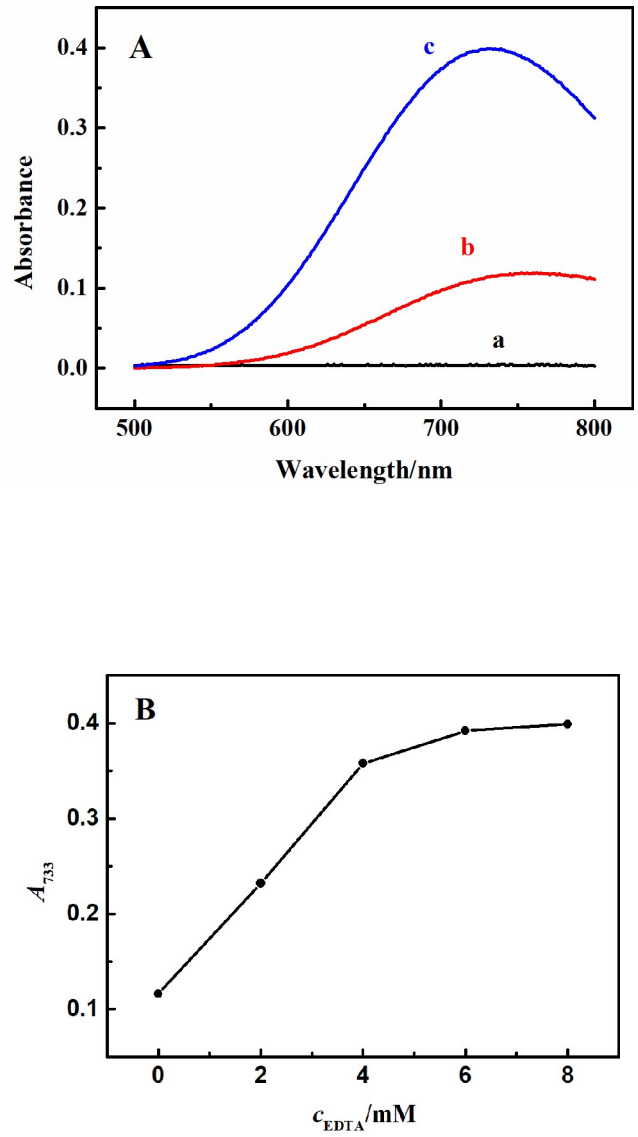


**Fig. S7** (A) UV-vis absorption spectra for Eu(III)-PMAG films in pH 5.0 buffers containing (a) 0, (b) 5.0 mM and (c) 5.0 mM Cu(II) + 8.0 mM EDTA. (B) Dependence of the $A_{733}$ for Eu(III)-PMAG films after immersion in pH 5.0 buffers containing 5.0 mM Cu(II) upon different EDTA concentrations ($c_{EDTA}$).

### 3.3 NADH-sensitive FL for Eu(III)-PMAG films

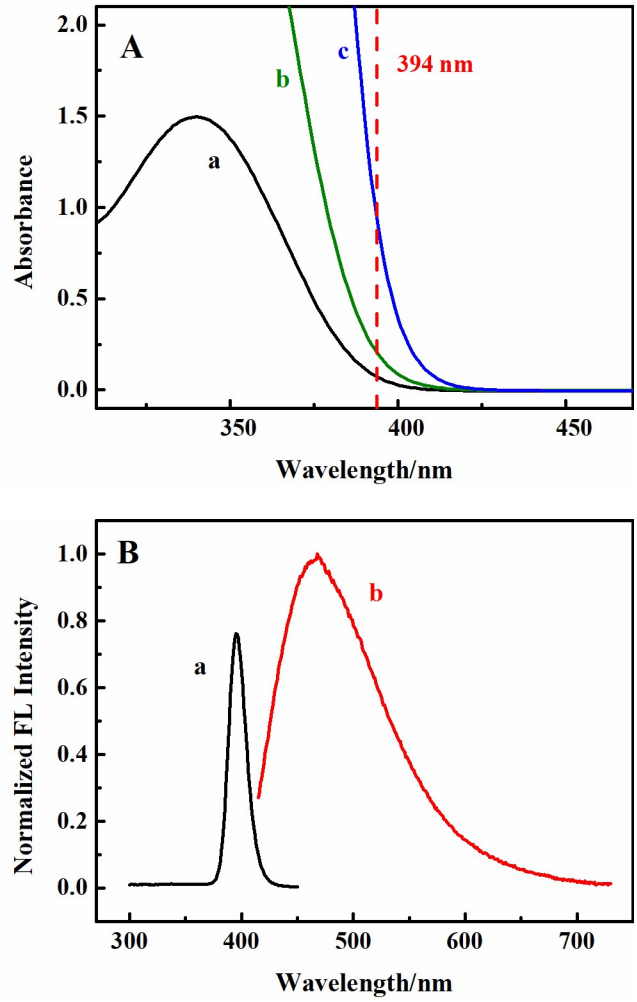


**Fig. S8** (A) UV-vis absorption spectra of (a) 0.5, (b) 1.0 and (c) 5.0 mM NADH in pH 5.0 buffers. (B) Fluorescence (a) excitation and (b) emission spectra ($\lambda_{ex}$ = 396 nm) of 5.0 mM NADH in pH 5.0 buffers.

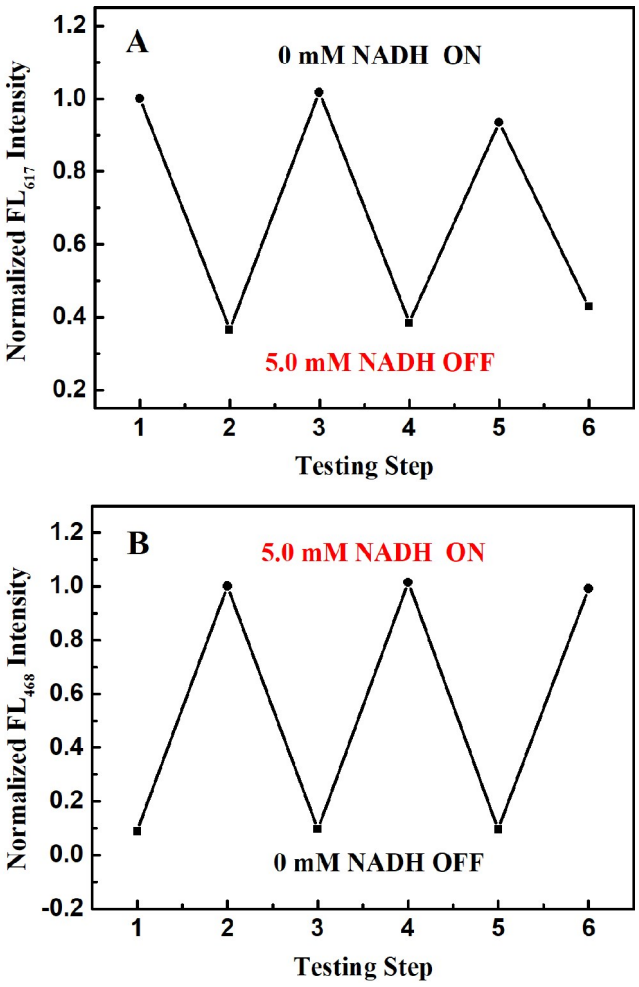


**Fig. S9** Variation of (A) $FL_{617}$ and (B) $FL_{468}$ for Eu(III)-PMAG films in pH 5.0 buffers with the NADH concentration switched between 0 and 5.0 mM.

### 3.5 Establishment of a 4-input/10-output logic gate

**Table S1** Truth table of the 4-input/10-output logic gate circuit

| Input A (Cu(II)) | Input B (EDTA) | Input C (NADH) | Input D (FcDA) | Output $FL_1$ | Output $FL_2$ | Output $FL_3$ | Output $FL_4$ | Output $IP_1$ | Output $IP_2$ | Output $IP_3$ | Output $AB_1$ | Output $AB_2$ | Output $AB_3$ |
|---|---|---|---|---|---|---|---|---|---|---|---|---|---|
| 0 | 0 | 0 | 0 | 1 | 0 | 0 | 0 | 0 | 0 | 1 | 0 | 0 | 1 |
| 1 | 0 | 0 | 0 | 0 | 1 | 0 | 0 | 0 | 0 | 1 | 0 | 1 | 0 |
| 0 | 1 | 0 | 0 | 1 | 0 | 0 | 0 | 0 | 0 | 1 | 0 | 0 | 1 |
| 1 | 1 | 0 | 0 | 1 | 0 | 0 | 0 | 0 | 0 | 1 | 1 | 0 | 0 |
| 0 | 0 | 1 | 0 | 0 | 0 | 1 | 1 | 0 | 0 | 1 | 0 | 0 | 1 |
| 1 | 0 | 1 | 0 | 0 | 0 | 1 | 1 | 0 | 0 | 1 | 0 | 1 | 0 |
| 0 | 1 | 1 | 0 | 0 | 0 | 1 | 1 | 0 | 0 | 1 | 0 | 0 | 1 |
| 1 | 1 | 1 | 0 | 0 | 0 | 1 | 1 | 0 | 0 | 1 | 1 | 0 | 0 |
| 0 | 0 | 0 | 1 | 1 | 0 | 0 | 0 | 0 | 1 | 0 | 0 | 0 | 1 |
| 1 | 0 | 0 | 1 | 0 | 1 | 0 | 0 | 0 | 1 | 0 | 0 | 1 | 0 |
| 0 | 1 | 0 | 1 | 1 | 0 | 0 | 0 | 0 | 1 | 0 | 0 | 0 | 1 |
| 1 | 1 | 0 | 1 | 1 | 0 | 0 | 0 | 0 | 1 | 0 | 1 | 0 | 0 |
| 0 | 0 | 1 | 1 | 0 | 0 | 1 | 1 | 1 | 0 | 0 | 0 | 0 | 1 |
| 1 | 0 | 1 | 1 | 0 | 0 | 1 | 1 | 1 | 0 | 0 | 0 | 1 | 0 |
| 0 | 1 | 1 | 1 | 0 | 0 | 1 | 1 | 1 | 0 | 0 | 0 | 0 | 1 |
| 1 | 1 | 1 | 1 | 0 | 0 | 1 | 1 | 1 | 0 | 0 | 1 | 0 | 0 |

### 3.6 Establishment of an encoder, a decoder, a demultiplexer and a parity checker

A

| Input C (NADH) | Input A (Cu(II)) | Output $FL_4$ |
|---|---|---|
| 0 | 1 | 0 |
| 1 | 0 | 1 |

B

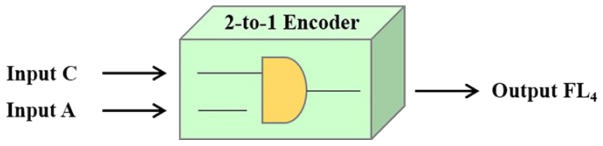


**Fig. S10** (A) Truth table and (B) logic symbol of a 2-to-1 encoder, employing NADH and Cu(II) as two inputs and $FL_{468}$ ($FL_4$) as the output.

A

| Input A (Cu(II)) | Output $FL_1$ | Output $AB_2$ |
|---|---|---|
| 0 | 1 | 0 |
| 1 | 0 | 1 |

B

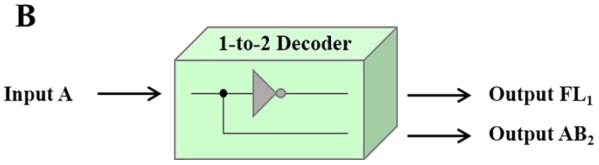


**Fig. S11** (A) Truth table and (B) logic symbol of a 1-to-2 decoder, employing Cu(II) as the input and $FL_{617}$ ($FL_1$) and $A_{733}$ ($AB_2$) as outputs.

### 3.8 Fabrication of the dual transfer gate

A

| Input A (Cu(II)) | Input D (FcDA) | Output $FL_2$ | Output $IP_2$ |
|---|---|---|---|
| 0 | 0 | 0 | 0 |
| 1 | 0 | 1 | 0 |
| 0 | 1 | 0 | 1 |
| 1 | 1 | 1 | 1 |

B

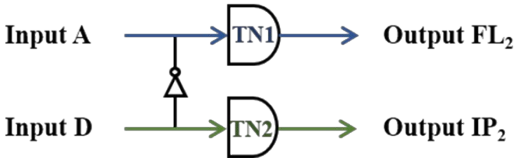


**Fig. S12** (A) Truth table and (B) symbolic representation of the dual transfer gate, employing Cu(II) and FcDA as inputs and $FL_{617}$ ($FL_2$) and CV $I_{pa}$ at 0.5 V ($IP_2$) as outputs.